Long-range allosteric transitions in carbamoyl phosphate synthetase

JAMES B. THODEN,[1] XINYI HUANG,[2,3] JUNGWOOK KIM,[2] FRANK M. RAUSHEL,[2] AND HAZEL M. HOLDEN[1]

[1]Department of Biochemistry, University of Wisconsin, Madison, Wisconsin 53706, USA
[2]Department of Chemistry, Texas A&M University, College Station, Texas 77843, USA

(RECEIVED April 20, 2004; FINAL REVISION May 24, 2004; ACCEPTED May 24, 2004)

Abstract

Carbamoyl phosphate synthetase plays a key role in both pyrimidine and arginine biosynthesis by catalyzing the production of carbamoyl phosphate from one molecule of bicarbonate, two molecules of MgATP, and one molecule of glutamine. The enzyme from *Escherichia coli* consists of two polypeptide chains referred to as the small and large subunits, which contain a total of three separate active sites that are connected by an intramolecular tunnel. The small subunit harbors one of these active sites and is responsible for the hydrolysis of glutamine to glutamate and ammonia. The large subunit binds the two required molecules of MgATP and is involved in assembling the final product. Compounds such as L-ornithine, UMP, and IMP allosterically regulate the enzyme. Here, we report the three-dimensional structure of a site-directed mutant protein of carbamoyl phosphate synthetase from *E. coli*, where Cys 248 in the small subunit was changed to an aspartate. This residue was targeted for a structural investigation because previous studies demonstrated that the partial glutaminase activity of the C248D mutant protein was increased 40-fold relative to the wild-type enzyme, whereas the formation of carbamoyl phosphate using glutamine as a nitrogen source was completely abolished. Remarkably, although Cys 248 in the small subunit is located at ~100 Å from the allosteric binding pocket in the large subunit, the electron density map clearly revealed the presence of UMP, although this ligand was never included in the purification or crystallization schemes. The manner in which UMP binds to carbamoyl phosphate synthetase is described.

Keywords: X-ray crystallography; protein structure; nucleotide binding; substrate channeling; amidotransferase; pyrimidine biosynthesis; arginine biosynthesis

Carbamoyl phosphate synthetase (CPS), a remarkably complex enzyme, belongs to a growing list of proteins with multiple active sites connected by internal molecular tunnels for the passage of reaction intermediates (Raushel et al. 2003). It catalyzes the formation of carbamoyl phosphate via a mechanism that requires four separate chemical reactions as outlined in Scheme 1 (Raushel et al. 1978; Raushel and Villafranca 1979).

The protein from *Escherichia coli* is composed of two dissimilar subunits as shown in Figure 1 (Thoden et al. 1997). The smaller subunit catalyzes the hydrolysis of glutamine to glutamate and ammonia, whereas the larger subunit contains two homologous active sites that are responsible for the overall synthesis of carbamoyl phosphate from ammonia, bicarbonate, and two molecules of MgATP. The active site within the N-terminal half of the large subunit (shown in green and referred to as the carboxy phosphate domain) catalyzes the phosphorylation of bicarbonate to carboxy phosphate and the subsequent reaction with ammonia to form carbamate (Scheme 1). The active site within the

Reprint requests to: Hazel M. Holden, Department of Biochemistry, University of Wisconsin, Madison, WI, 53706, USA; e-mail: Hazel_Holden@biochem.wisc.edu; fax: (608) 262-1319; or Frank M. Raushel, Department of Chemistry, Texas A&M University, College Station, TX 77843, USA; e-mail: Raushel@tamu.edu; fax: (979) 845-9452.

[3]Present address: Wyeth Research, Biophysics/Enzymology Group, Chemical and Screening Sciences, 401 North Middleton Road, Pearl River, NY 10965, USA.

Article and publication date are at http://www.proteinscience.org/cgi/doi/10.1110/ps.04822704.

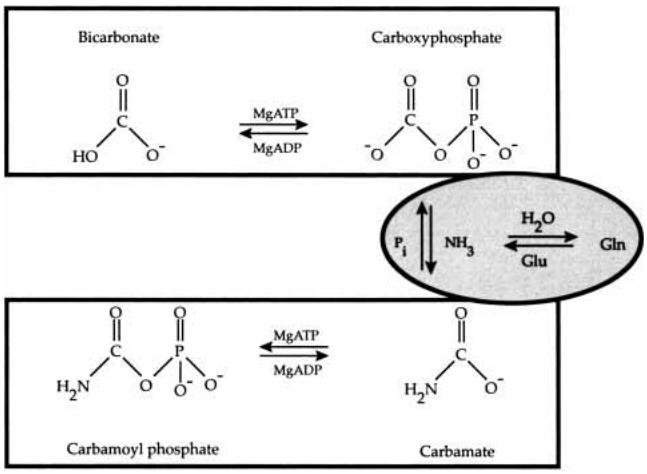

Scheme 1

C-terminal half of the large subunit (shown in blue and referred to as the carbamoyl phosphate domain) catalyzes the phosphorylation of carbamate to the ultimate product, carbamoyl phosphate.

Two molecular tunnels connect the three active sites contained within the small and large subunits (Fig. 1). The ammonia tunnel extends from the active site of the small subunit to the active site of the carboxy phosphate domain. The carbamate tunnel connects the two active sites within the large subunit. In support of the existence of these tunnels, isotope-labeling studies have demonstrated that ammonia, produced from the hydrolysis of glutamine, does not dissociate into the bulk solvent from the small subunit and then rebind to the large subunit (Mullins and Raushel 1999). The functional significance of these tunnels has also been probed by the construction of appropriate site-directed mutant proteins and characterization of their respective kinetic parameters (Huang and Raushel 2000a,b). Of particular significance are the site-directed mutagenesis studies targeting Gly 359 of the small subunit, which forms part of the ammonia tunnel. These investigations revealed an uncoupling of the partial reactions catalyzed by CPS, specifically the hydrolysis of glutamine and MgATP, upon substitution of glycine with bulkier side-chain moieties. To further probe the structural consequences of replacing Gly 359 with various amino acid side chains, the G359F mutant enzyme was crystallized and its structure solved to 2.1 Å resolution (Thoden et al. 2002). The substitution of glycine with a phenylalanine resulted in the perturbation of the polypeptide-chain backbone conformation beginning at Pro 354. This conformational change resulted in the formation of an escape route for the ammonia through a pathway leading directly to the bulk solvent.

From extensive biochemical data, it is now known that a fully coupled CPS requires the hydrolysis of one glutamine and the utilization of two molecules of MgATP for every molecule of carbamoyl phosphate formed. The three active sites of the enzyme must therefore be synchronized with one another in order to maintain the overall stoichiometry of the reaction without the wasteful hydrolysis of glutamine and/or MgATP. The initial rate of formation of the carboxy phosphate intermediate does not depend upon the binding or hydrolysis of glutamine within the small subunit. In contrast, the hydrolysis of glutamine is accelerated by ~1000-fold upon the phosphorylation of bicarbonate (Miles and Raushel 2000). The formation of the carboxy phosphate intermediate thus serves as a trigger for the hydrolysis of glutamine (Miles and Raushel 2000). Apparently, ammonia does not migrate through the molecular tunnel toward the large subunit until after the carboxy phosphate intermediate has been formed. These data also suggest that the phosphorylation of bicarbonate within the large subunit induces a conformational change that must be allosterically transmitted to the small subunit.

Anderson and coworkers obtained some of the earliest experimental support for conformational changes induced by the reaction of MgATP and bicarbonate within the carboxy phosphate domain (Foley et al. 1971). These investigators discovered that a specific sulfhydryl group within the small subunit of CPS could be labeled with N-ethyl maleimide (NEM) only when MgATP and bicarbonate were also included in the reaction mixture. This cysteine residue must therefore be inaccessible for reaction with NEM in the

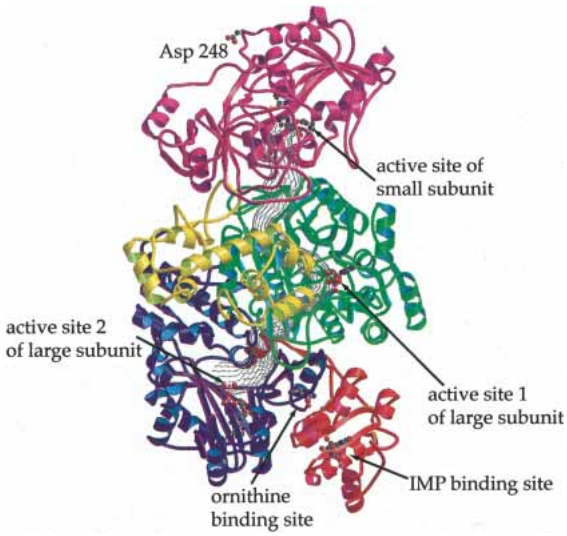

Figure 1. Ribbon representation of the CPS α,β-heterodimer. The small subunit is shown in magenta. The large subunit is color coded in green, yellow, blue, and red to indicate those regions defined by Met 1 to Glu 403, Val 404 to Ala 553, Asn 554 to Asn 936, and Ser 937 to Lys 1073, respectively. In the presence of allosteric activators such as L-ornithine, α,β-heterodimers associate to form an $(\alpha,\beta)_4$-tetrameric species. The green and blue portions of the large subunit are referred to as the carboxy phosphate and carbamoyl phosphate domains. The tunnel connecting the three active sites is depicted in a gray chicken wire representation. The position of the C248D mutation in the small subunit is indicated.

absence of MgATP and bicarbonate. However, in the presence of MgATP and bicarbonate, the conformation of the protein in the vicinity of this cysteine must be altered to the point where the thiol group can be efficiently labeled with NEM. Once labeled with NEM, the glutaminase reaction is accelerated by 20- to 30-fold, and the rate of MgATP hydrolysis is reduced. The labeling of this cysteine residue within the small subunit with NEM apparently traps CPS in a conformation that resembles the complex activated by the formation of the carboxy phosphate intermediate. The specific cysteine residue in the small subunit was subsequently identified as Cys 248 through site-directed mutagenesis experiments (Mareya and Raushel 1994). This cysteine is ~50 Å away from the binding site for MgATP and bicarbonate in the carboxy phosphate domain of the large subunit. The substitution of Cys 248 with an aspartate residue was shown to closely mimic the catalytic properties of the NEM-labeled enzyme. The partial glutaminase activity was increased 40-fold relative to the wild-type enzyme, whereas the formation of carbamoyl phosphate using glutamine as a nitrogen source was completely abolished. These results suggest that replacement of Cys 248 with other residues can

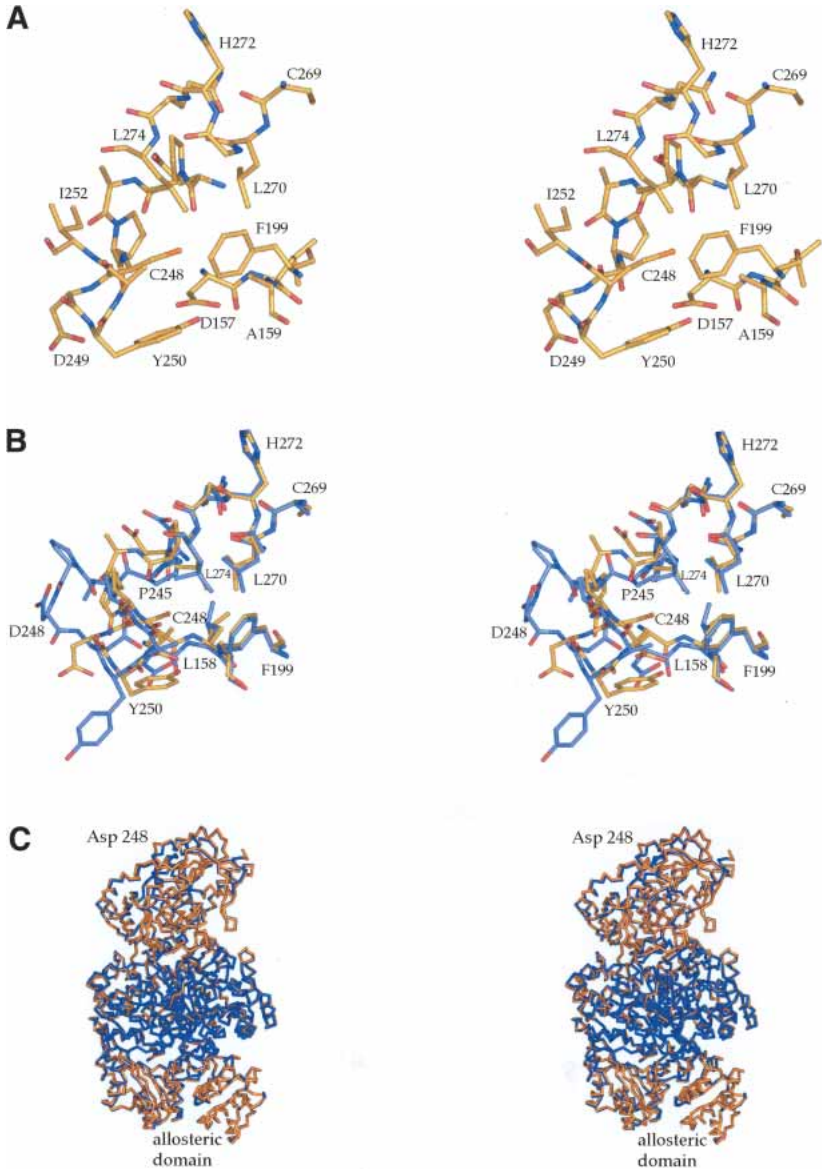

Figure 2. The site of mutation in the small subunit. A close-up view of the region surrounding Cys 248 in the small subunit of the wild-type protein is presented in *A*. X-ray coordinates used for this figure were from the Protein Data Bank (1JDB). *(B)* A superposition of the region near the site of the mutation for the wild-type and the C248D proteins is shown. The wild-type and mutant protein structures are depicted in yellow and blue, respectively. *(C)* A superposition of the polypeptide-chain traces for the wild-type and the C248D mutant proteins depicted in blue and gold, respectively.

induce conformational changes in the small subunit that resemble those that are predicted to occur upon the phosphorylation of bicarbonate by MgATP within the large subunit. Note that this cysteine residue is not conserved among carbamoyl phosphate synthetases, although the residues preceding it (Ser-Asn-Gly-Pro-Gly-Asp-Pro) appear to be highly conserved.

The activation of the glutaminase activity cannot be induced by the binding of analogs of MgATP and MgADP. Therefore, it appears that the formation of the carboxy phosphate intermediate is required for the induction of the conformational and/or dynamic changes that must be transmitted to the amidotransferase domain of CPS. Because the carboxy phosphate is very unstable (Sauers et al. 1975), it would be difficult to determine the transient conformational changes that occur within the small subunit. In an attempt to overcome these issues, we report here the three-dimensional structure of the C248D mutant protein crystallized in the presence of MnADP and L-ornithine. Strikingly, the C248D mutant protein was shown to bind UMP in the allosteric binding pocket of the large subunit, although no such nucleotide was included in the purifications or crystallization trials.

Results and Discussion

The position of the C248D mutation in the small subunit of CPS, relative to the large subunit, can be seen from Figure 1. This amino acid residue is located at ~50 Å from the binding sites for MgATP and bicarbonate, located within the carboxy phosphate domain of the CPS large subunit. In the wild-type protein, Cys 248 resides at the start of an α-helix with its side-chain sulfhydryl group buried in a reasonably hydrophobic pocket as shown in Figure 2A. The sulfur of Cys 248 lies at ~11 Å from the sulfur of the active site cysteine (Cys 269). Quite strikingly, the aliphatic side chain of Leu 270 is wedged between these two sulfhydryl groups.

Electron density corresponding to the site of the C248D mutation is shown in Figure 3A. Whereas the polypeptide chain backbone is well defined, the electron density corresponding to the aspartate side chain is somewhat weak. The dramatic changes that occur in the course of the polypeptide chain upon substitution of Cys 248 with an aspartate residue are highlighted in Figure 2B. The positions of the α-carbons for Cys 248 in the wild-type enzyme versus Asp 248 in the mutant protein differ by ~6.0 Å. Significant changes in the polypeptide chains for the wild-type and mutant proteins, however, are not confined to residue 248, but rather are propagated throughout the region defined by Gly 243 to Ala 251. In the wild-type enzyme, Pro 245 adopts ϕ, ψ angles of −81°, and −38°, respectively, which is in sharp contrast to that observed for the C248D mutant protein, whereby the corresponding angles are −80° and 144°. These types of

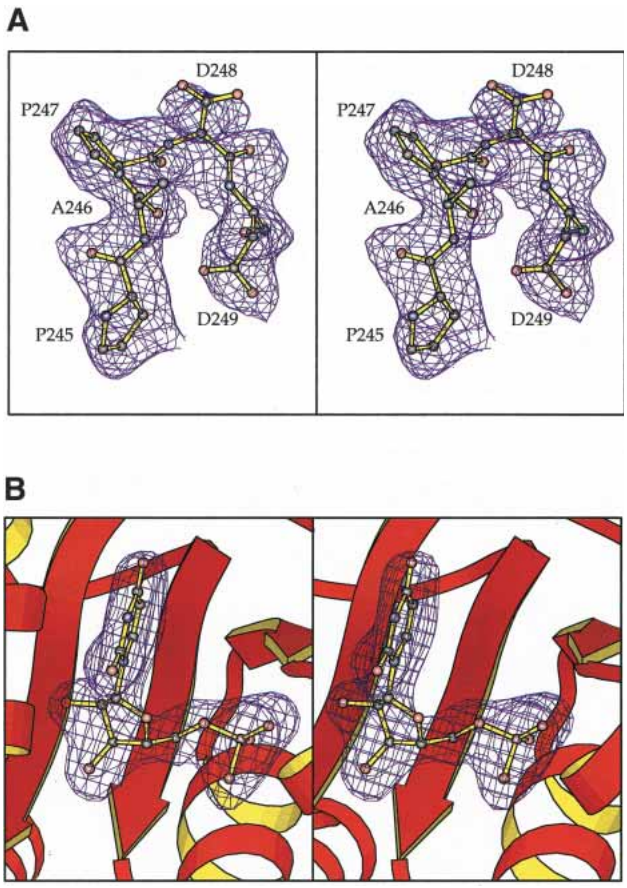

Figure 3. Representative electron density. The region near the site of the C248D mutation is shown in *A*, whereas the electron density corresponding to the bound UMP is displayed in *B*. The electron density maps shown were calculated with coefficients of the form (F_o - F_c) and contoured at 3σ.

differences in dihedral angles between the two models continue until Tyr 250. The α-carbons for Gly 243 to Ala 251 in the wild-type and C248D mutant proteins superimpose with a root-mean-square deviation of ~2.0 Å. As a consequence of these perturbations, the side chain of Asp 248 is solvent exposed, as can be seen in Figure 1. Excluding the region between Gly 243 to Ala 251, however, the α-carbons for the wild-type and C248D mutant proteins correspond with a root-mean-square deviation of 0.27 Å according to the algorithm of Cohen (1997). As can be seen in Figure 2C, no major domain movements are observed between the two protein models.

Although caution must be applied in interpreting the significance of temperature factors, it is noteworthy that in the wild-type protein, the average B-factor for all atoms between Gly 243 and Ala 251 is ~45 $Å^2$, whereas for the mutant protein, the average B-factor is considerably higher at ~90 $Å^2$. Clearly the substitution of an aspartate residue for the buried cysteine at position 248 creates conformational flexibility within this area of the small subunit.

Within coordinate error, the geometries for the three active sites of the wild-type enzyme and the C248D mutant protein are virtually identical. Additionally, within the small subunit, the relative positions and temperature factors for Ser 47, Cys 269, His 353, and Glu 355, all of which play key roles in glutamine hydrolysis, are similar in the wild-type and mutant proteins.

UMP, a product of pyrimidine biosynthesis, is known to allosterically inhibit CPS. This mode of inhibition is primarily through modulation of the Michaelis constant for MgATP (Braxton et al. 1992, 1996). IMP is also known to bind to CPS and was originally described as an activator (Boettcher and Meister 1981, 1982; Kasprzak and Villafranca 1988). More recent investigations have demonstrated, however, that the effects of IMP on CPS activity can be modulated by temperature (Braxton et al. 1992). An X-ray analysis of CPS in the presence of both IMP and L-ornithine revealed unequivocally the location of the binding pocket for the nucleotide as indicated in Figure 1 (Thoden et al. 1999). The IMP moiety is positioned at the C-terminal portion of a five-stranded parallel β-sheet and is anchored to the protein via Lys 954, Thr 974, Thr 977, Lys 993, Asn 1015, and Thr 1017 as shown schematically in Figure 4A. Strikingly, only the peptidic NH group of Val 994 forms a hydrogen-bonding interaction with the hypoxanthine base of the ligand. A series of hydrogen bonds connects the IMP-binding pocket to the active site of the carbamoyl phosphate domain in the large subunit. In that the allosteric effects exhibited by IMP and UMP are strictly competitive with one another, it has been speculated that UMP binds in a similar position to that observed for IMP (Braxton et al. 1999). To date, however, all of the structures known of CPS have been solved in the presence of L-ornithine, potassium ions, and various combinations of MnADP or ATP-analogs. It has not been possible to obtain crystals of CPS with only UMP bound to the enzyme.

The C248D mutant protein presented here was crystallized in the presence of L-ornithine, potassium ions, and MnADP. Surprisingly, as the model was being refined, it became apparent that UMP was bound in the allosteric pocket, although no UMP had been included in the purifications or crystallization trials. Electron density corresponding to the UMP ligand is shown in Figure 3B. The apparent dissociation constant for the binding of UMP to the C248D mutant protein was found to be 9 μM. This value is approximately threefold larger than the dissociation constant obtained under the same conditions for UMP binding to the wild-type enzyme. Therefore, the unexpected finding of UMP bound to the allosteric domain of CPS cannot be explained on the basis of a significant enhancement in the affinity of UMP for the enzyme. Strikingly, the site of the C248D mutation is ~100 Å from the allosteric binding pocket of the large subunit, and whereas it is not apparent from the present crystal structure why UMP bound, nonetheless, these results underscore the intricate interplay among the various tertiary structural elements defining the molecular architecture of CPS.

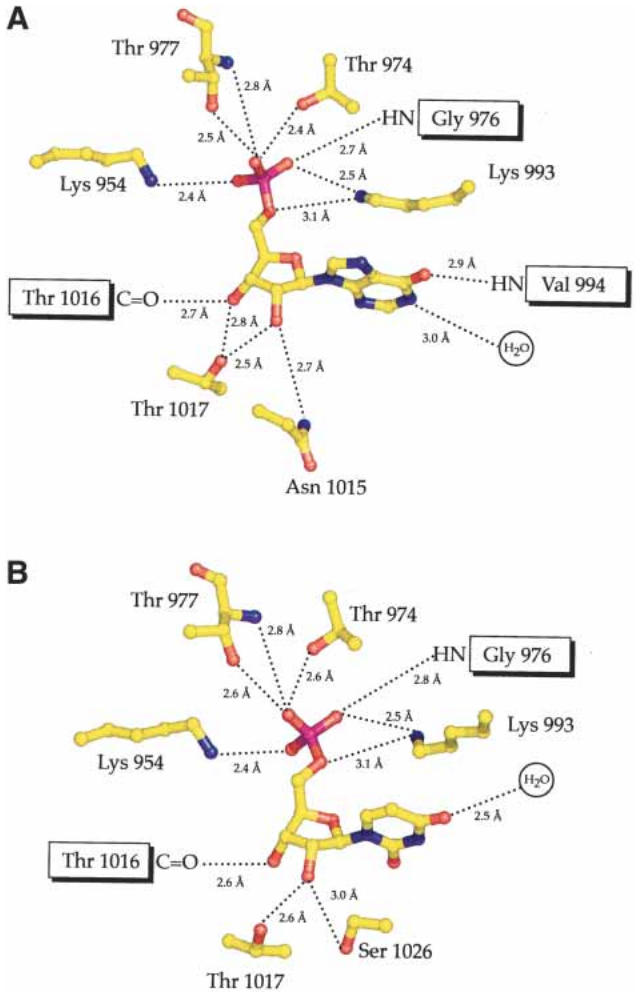

Figure 4. Electrostatic interactions between CPS and the IMP or UMP ligands. Schematic representations of the hydrogen bonding patterns between the protein and the IMP and UMP ligands are depicted in *A* and *B*, respectively.

Regardless of the manner in which UMP found its way into the allosteric domain during protein expression, those key chemical interactions that allow for its binding to CPS can still be addressed. The one caveat, however, is that the observed binding mode of UMP to CPS is that for the activated species, and there may be some subtle but important differences when UMP is bound to the enzyme in the absence of L-ornithine.

UMP binds to CPS in a quite solvent-exposed region. A close-up view of the allosteric domain within ~5 Å of the UMP ligand is given in Figure 5A. The uracil ring of the nucleotide adopts the anticonformation, whereas the ribose assumes the $C_{2'}$-*endo* pucker. Both Lys 954 and Lys 993

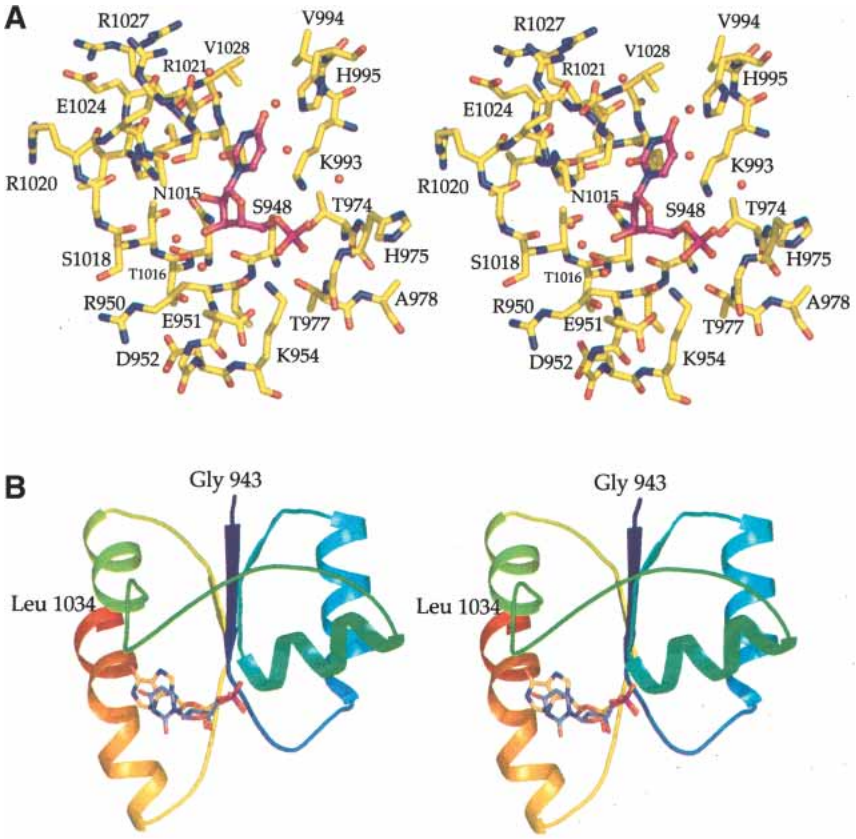

Figure 5. Binding of UMP to CPS. Those amino acid residues lying within ~5.0 Å of the UMP moiety are shown in *A*. A superposition of the UMP and IMP ligands, displayed in blue and yellow, respectively, is shown in *B*.

play key roles in nucleotide binding by providing electrostatic interactions with the phosphoryl group of the ligand. A superposition of the IMP versus UMP ligand is presented in Figure 5B in context of tertiary structure. There are limited conformational changes that occur upon the binding of either nucleotide, such that the α-carbons for the allosteric domains of CPS with bound UMP or IMP superimpose with a root-mean-square deviation of 0.19 Å. As indicated in the schematic representations presented in Figure 4, A and B, the anchoring of the phosphoryl group of UMP or IMP to CPS is nearly identical. The ribose C5-oxygens of the two ligands, however, are separated by ~1.4 Å, with the net result that in IMP, the base is somewhat more buried as compared with UMP (Fig. 5B). This difference in ribose binding is reflected in the somewhat different hydrogen-bonding interactions around the sugar hydroxyl groups (Fig. 4). Interestingly, recent site-directed mutagenesis experiments targeted at Ser 948, Asn 1015, Thr 1017, and Ser 1026 have demonstrated that the mutation of Ser 1026 to an alanine has a much larger effect on the binding of IMP versus the binding of UMP (Pierrat and Raushel 2002). Perhaps the most notable difference between IMP versus UMP binding is the hydrogen-bonding pattern around the bases. In the case of IMP, the hypoxanthine moiety is linked to the protein via the peptidic NH group of Val 994. In UMP, the distance between the C4 carbonyl oxygen of the base and the peptidic NH group of Val 994 is 4.6 Å. There are no interactions within 3.6 Å between the protein and the uracil base.

The synchronization of multiple chemical reactions within the three active sites of CPS requires the propagation of allosteric signals from one catalytic domain to another. In CPS, the dominant active site is likely to be the one responsible for the generation of the carboxy phosphate intermediate in the large subunit. The initial rate of bicarbonate phosphorylation is apparently independent of catalytic or binding events that occur within the small subunit of CPS. However, the phosphorylation of bicarbonate enhances the hydrolysis rate of glutamine by approximately three orders of magnitude. This observation requires that a conformational change or an alteration in structural dynamics must be transmitted from the large subunit to the small subunit. These alterations within the small subunit thus serve to enhance the inherent catalytic activity required to hydrolytically liberate ammonia from the side-chain carboxamide of glutamine. The magnitude of these structural perturbations that occur within the small subunit is unknown.

Table 1. *X-ray data collection statistics*

Data set	Resolution (Å)	Independent reflections	Completeness (%)	Redundancy	AvgI/Avg σ(I)	R_{sym}[a]
	30.0–2.10	433843	90.0	2.7	15.2	4.8
	2.18 ± 2.10[b]	39976	83.0	2.3	3.3	20.3

[a] $R_{sym} = (\sum|I - \bar{I}|/\sum I) \times 100$.
[b] Statistics for the highest resolution bin.

The catalytic properties of the C248D mutation within the small subunit of CPS are consistent with an altered conformational state that may mimic the activated form of the small subunit, which is likely to occur upon the formation of the carboxy phosphate intermediate within the large subunit. Relative to the wild-type enzyme, there are significant alterations immediately around the site of the mutation. In addition, the carboxylate side chain of the aspartate is now exposed to solvent rather than buried within a hydrophobic pocket. This region of the mutant protein also appears to be conformationally less rigid than the wild-type enzyme. However, the conformational changes that can be identified among those residues that are directly involved in the hydrolysis or binding of glutamine are relatively small. These results suggest that either the mutant structure is a rather poor mimic of the activated complex that is thought to occur, or that the specific perturbations to the active site of the small subunit need not be so dramatic as to be readily detected within the limits of X-ray crystallography. Alternatively, the enhancement in the rate of glutamine hydrolysis may occur within complexes that are formed only after the binding of glutamine to the active site. Stable analogs of the carboxy phosphate intermediate are being synthesized in an attempt to provide a more realistic mimic of the chemical events that trigger the conformational and/or dynamic perturbations that must be allosterically transmitted to the small subunit.

Materials and methods

Crystallization procedures

The C248D mutant of the small subunit of CPS was prepared and purified to homogeneity as previously described (Mareya and Raushel 1994). Large single crystals were grown at 4°C by batch from 8% poly(ethylene glycol) 8000, 0.65 M tetraethylammonium chloride, 0.5 mM $MnCl_2$, 100 mM KCl, 1.5 mM ADP, 25 mM HEPPS (pH 7.4), and 0.5 mM L-ornithine. Once the crystals reached dimensions of ~0.3 mm × 0.3 mm × 0.8 mm, they were flash-frozen according to previously published procedures (Thoden et al. 1997) and stored under liquid nitrogen until synchrotron beam time became available. The crystals belonged to the space group $P2_12_12_1$ with unit cell dimensions of $a = 151.1$ Å, $b = 164.2$ Å, and $c = 331.5$ Å and one complete $(\alpha,\beta)_4$-heterotetramer per asymmetric unit.

X-ray data collection and processing

An X-ray data set for the C248D mutant protein was collected on a 3 × 3 tiled "SBC2" CCD detector at the Structural Biology Center 19-ID Beamline (Advanced Photon Source, Argonne National Laboratory). The data were processed with HKL2000 and scaled with SCALEPACK (Otwinowski and Minor 1997). Relevant data collection statistics are presented in Table 1. The structure of the C248D mutant protein was solved by Difference Fourier techniques to a nominal resolution of 2.1 Å using X-ray coordinates deposited in the Protein Data Bank under 1JDB. The initial model was subjected to least-squares refinement with the software package TNT (Tronrud et al. 1987), which reduced the overall *R*-factor to 26.8%. To expedite the structure-refinement process, the electron densities corresponding to the four α,β-heterodimers in the asymmetric unit were averaged with the program AVE in the RAVE suite of programs and the "averaged" model adjusted according to the map (Jones 1992; Kleywegt and Jones 1994). This averaging and rebuilding process lowered the overall *R*-factor to 21.0%. Next, the "averaged" model was used to create the entire $(\alpha,\beta)_4$-heterotetramer, which was placed back into the unit cell. Maps were calculated with coefficients of the form $(2F_o - F_c)$, where F_o was the native structure factor amplitude and F_c was the calculated structure factor amplitude from the model. The four α,β-heterodimers in the asymmetric unit were adjusted to the electron density using the program TURBO (Roussel et al. 1990). The

Table 2. *Relevant refinement statistics*

Resolution limits (Å)	30.0–2.10
[a]*R*-factor (overall) %/no. reflections	17.9/430,365
R-factor (working) %/no. reflections	17.6/387,352
R-factor (free) %/no. reflections	20.9/42551
No. protein atoms	44,392[b]
No. hetero-atoms	4365[c]
Bond lengths (Å)	0.012
Bond angles (deg)	2.43
Trigonal planes (Å)	0.006
General planes (Å)	0.013
Torsional angles (deg)[d]	17.8

[a] *R*-factor $= (\sum|F_o - F_c|/\sum|F_o|) \times 100$ where F_o is the observed structure-factor amplitude and F_c is the calculated structure-factor amplitude.
[b] These include multiple conformations for K80, R130, R425, R490, E512, E549, M772, Q967, and R1027 in Subunit A; M60, K423, Q491, E591, D758, E804, Q967, and N1007 in Subunit C; R148 in Subunit D; S29, E39, K515, Q645, and Q967 in Subunit E; and E153, S414, R426, K475, Q645, R652, Q967, and E1009 in Subunit G.
[c] These include 22 potassium ions, 12 manganese(II) ions, 27 chloride ions, 4 tetraethyl ammonium ions, 8 ADP molecules, 4 UMP molecules, 4 L-ornithines, and 3907 water molecules.
[d] The torsional angles were not restrained during the refinement.

final *R*-factor was 18.0% for all measured X-ray data. Relevant refinement statistics are given in Table 2. Note that the α-carbons for each of the four α,β-heterodimers in the asymmetric unit superimpose upon one another with typical root-mean-square deviations ranging from 0.18 Å to 0.22 Å. Within experimental error, these α,β-heterodimers are identical, and thus the results described here refer to the first α,β-heterodimer in the X-ray coordinate file deposited in the Research Collaboratory for Structural Bioinformatics.

Measurement of the apparent dissociation constant

The apparent dissociation constant for the binding of UMP to CPS was measured by a determination of the effect of UMP on the partial back reaction as described in Pierrat and Raushel (2002).

Acknowledgments

Use of the Argonne National Laboratory Structural Biology Center beamlines at the Advanced Photon Source was supported by the U.S. Department of Energy, Office of Energy Research, under contract no. W-31-109-ENG-38. This research was supported in part by grants from the NIH (GM55513 to H.M.H. and DK30343 to F.M.R.) and the Robert A. Welch Foundation (A840). X-ray coordinates have been deposited in the Research Collaboratory for Structural Bioinformatics, Rutgers University, New Brunswick, N.J. (1T36) and will be released upon publication.

The publication costs of this article were defrayed in part by payment of page charges. This article must therefore be hereby marked "advertisement" in accordance with 18 USC section 1734 solely to indicate this fact.

References

Boettcher, B. and Meister, A. 1981. Conversion of UMP, an allosteric inhibitor of carbamyl phosphate synthetase, to an activator by modification of the UMP ribose moiety. *J. Biol. Chem.* **256:** 5977–5980.

———. 1982. Regulation of *Escherichia coli* carbamyl phosphate synthetase. Evidence for overlap of the allosteric nucleotide binding sites. *J. Biol. Chem.* **257:** 13971–13976.

Braxton, B.L., Mullins, L.S., Raushel, F.M., and Reinhart, G.D. 1992. Quantifying the allosteric properties of *Escherichia coli* carbamyl phosphate synthetase: Determination of thermodynamic linked-function parameters in an ordered kinetic mechanism. *Biochemistry* **31:** 2309–2316.

Braxton, B.L., Mullins, L.S., Raushel, F.M., and Reinhart, G.D. 1996. Allosteric effects of carbamoyl phosphate synthetase from *Escherichia coli* are entropy-driven. *Biochemistry* **35:** 11918–11924.

Braxton, B.L., Mullins, L.S., Raushel, F.M., and Reinhart, G.D. 1999. Allosteric dominance in carbamoyl phosphate synthetase. *Biochemistry* **38:** 1394–1401.

Cohen, G.H. 1997. ALIGN: A program to superimpose protein coordinates, accounting for insertions and deletions. *J. Appl. Crystal.* **30:** 1160–1161.

Foley, R., Poon, J., and Anderson, P.M. 1971. Characterization of the reactive sulfhydryl groups in carbamyl phosphate synthetase of *Escherichia coli*. *Biochemistry* **10:** 4562–4569.

Huang, X. and Raushel, F.M. 2000a. An engineered blockage within the ammonia tunnel of carbamoyl phosphate synthetase prevents the use of glutamine as a substrate but not ammonia. *Biochemistry* **39:** 3240–3247.

———. 2000b. Restricted passage of reaction intermediates through the ammonia tunnel of carbamoyl phosphate synthetase. *J. Biol. Chem.* **275:** 26233–26240.

Jones, T.A. 1992. A set of averaging programs. *Molecular Replacement* (eds. E. Dodson et al.), pp. 91–105. SERC Daresbury Laboratory, Warrington, UK.

Kasprzak, A.A. and Villafranca, J.J. 1988. Interactive binding between the substrate and allosteric sites of carbamoyl-phosphate synthetase. *Biochemistry* **27:** 8050–8056.

Kleywegt, G.J. and Jones, T.A. 1994. Halloween . . . masks and bones. *From first map to final model* (eds. S. Bailey et al.), pp. 59–66. SERC Daresbury Laboratory, Warrington, UK.

Mareya, S.M. and Raushel, F.M. 1994. A molecular wedge for triggering the amidotransferase activity of carbamoyl phosphate synthetase. *Biochemistry* **33:** 2945–2950.

Miles, B.W. and Raushel, F.M. 2000. Synchronization of the three reaction centers within carbamoyl phosphate synthetase. *Biochemistry* **39:** 5051–5056.

Mullins, L.S. and Raushel, F.M. 1999. Channeling of ammonia through the intermolecular tunnel contained within carbamoyl phosphate synthetase. *J. Amer. Chem. Soc.* **121:** 3803–3804.

Otwinowski, Z. and Minor, W. 1997. Processing of x-ray diffraction data collected in oscillation mode. *Methods Enzymol.* **276:** 307–326.

Pierrat, O.A. and Raushel, F.M. 2002. A functional analysis of the allosteric nucleotide monophosphate binding site of carbamoyl phosphate synthetase. *Arch. Biochem. Biophys.* **400:** 34–42.

Raushel, F.M. and Villafranca, J.J. 1979. Determination of rate-limiting steps of *Escherichia coli* carbamoyl-phosphate synthase. Rapid quench and isotope partitioning experiments. *Biochemistry* **18:** 3424–3429.

Raushel, F.M., Anderson, P.M., and Villafranca, J.J. 1978. Kinetic mechanism of *Escherichia coli* carbamoyl-phosphate synthetase. *Biochemistry* **17:** 5587–5591.

Raushel, F.M., Thoden, J.B., and Holden, H.M. 2003. Enzymes with molecular tunnels. *Acc. Chem. Res.* **36:** 539–548.

Roussel, A., Fontecilla-Camps, J.C., and Cambillau, C. 1990. *TURBO-FRODO*. *Acta Cryst. Sect. A* **4:** 66–67.

Sauers, C.K., Jencks, W.P., and Groh, S. 1975. The alcohol-bicarbonate-water system. Structure reactivity studies on the equilibria of alkyl monocarbonates and on the rates of their decomposition in aqueous alkali. *J. Amer. Chem. Soc.* **97:** 5546–5553.

Thoden, J.B., Holden, H.M., Wesenberg, G., Raushel, F.M., and Rayment, I. 1997. Structure of carbamoyl phosphate synthetase: A journey of 96 Å from substrate to product. *Biochemistry* **36:** 6305–6316.

Thoden, J.B., Raushel, F.M., Wesenberg, G., and Holden, H.M. 1999. The binding of inosine monophosphate to *Escherichia coli* carbamoyl phosphate synthetase. *J. Biol. Chem.* **274:** 22502–22507.

Thoden, J.B., Huang, X., Raushel, F.M., and Holden, H.M. 2002. Carbamoyl-phosphate synthetase. Creation of an escape route for ammonia. *J. Biol. Chem.* **277:** 39722–39727.

Tronrud, D.E., Ten Eyck, L.F., and Matthews, B.W. 1987. An efficient general-purpose least-squares refinement program for macromolecular structures. *Acta Crystallogr. Sect. A* **43:** 489–501.